Supporting Information

Activation of Periodate by Freezing for the Degradation of Aqueous Organic Pollutants

Yejin Choi,[†] Ho-Il Yoon,[‡] Changha Lee,[§] Ľubica Vetráková,[//] Dominik Heger,[//] Kitae Kim*[,‡,⊥], and Jungwon Kim*[,†]

[†]Department of Environmental Sciences and Biotechnology, Hallym University, Chuncheon, Gangwon-do 24252, Republic of Korea

[‡]Korea Polar Research Institute (KOPRI), Incheon 21990, Republic of Korea

[§]School of Urban and Environmental Engineering, Ulsan National Institute of Science and Technology (UNIST), Ulsan 44919, Republic of Korea

[//]Department of Chemistry and Research Centre for Toxic Compounds in the Environment (RECETOX), Faculty of Science, Masaryk University, Kamenice 5, 625 00 Brno, Czech Republic

[⊥]Department of Polar Sciences, University of Science and Technology (UST), Incheon 21990, Republic of Korea

Total 15 pages

Eqs S1−S5, Figures S1−S11, Discussion on the effect of cooling method on the induction period, and References

Corresponding Authors

*(K.K.) Phone: +82-32-760-5365; e-mail: ktkim@kopri.re.kr.

*(J.K.) Phone: +82-33-248-2156; e-mail: jwk@hallym.ac.kr.

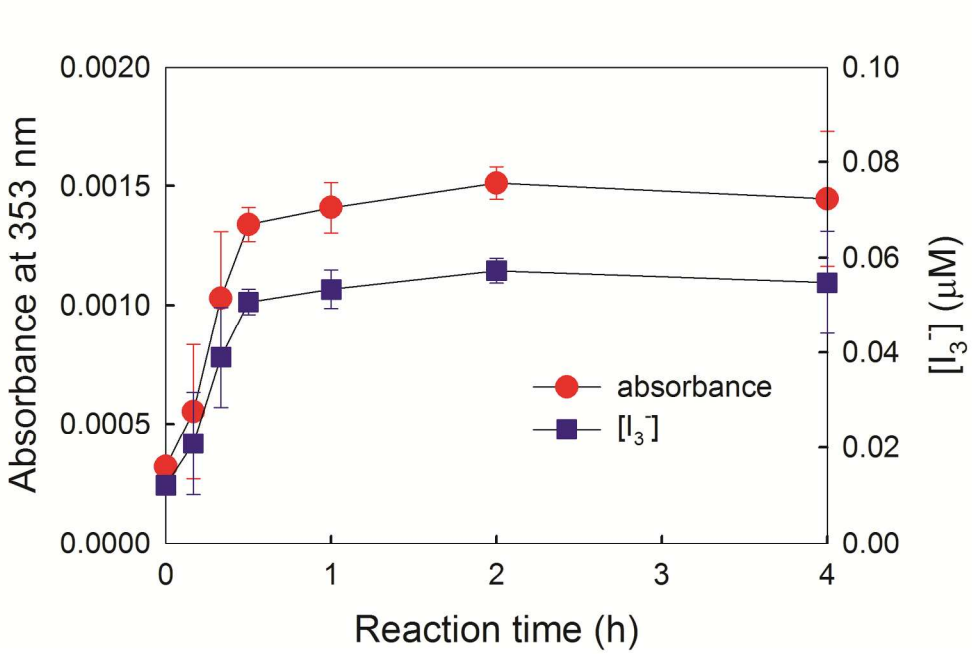

Figure S1. Time profiles of the increase of absorbance at 353 nm and the corresponding production of I_3^- in the presence of IO_4^- and FFA during freezing. Experimental conditions were as follows: [IO_4^-] = 100 μM, [FFA] = 20 μM, pH = 3.0, and freezing temperature = −20 °C. The concentration of I_3^- was calculated by assuming that the absorbance at 353 nm is only due to the generation of I_3^-.

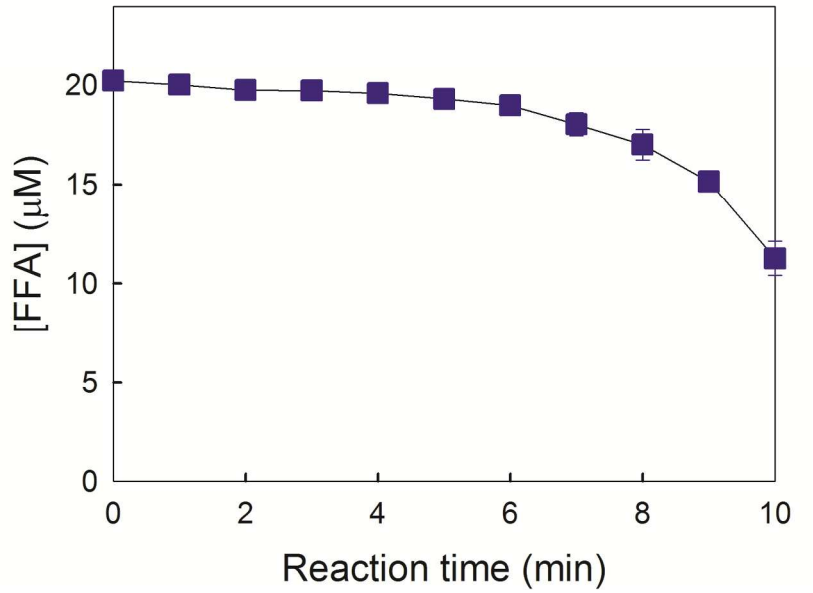

Figure S2. Degradation of FFA in the presence of IO_4^- during freezing. Experimental conditions were as follows: [IO_4^-] = 100 μM, [FFA] = 20 μM, pH = 3.0, and freezing temperature = −20 °C.

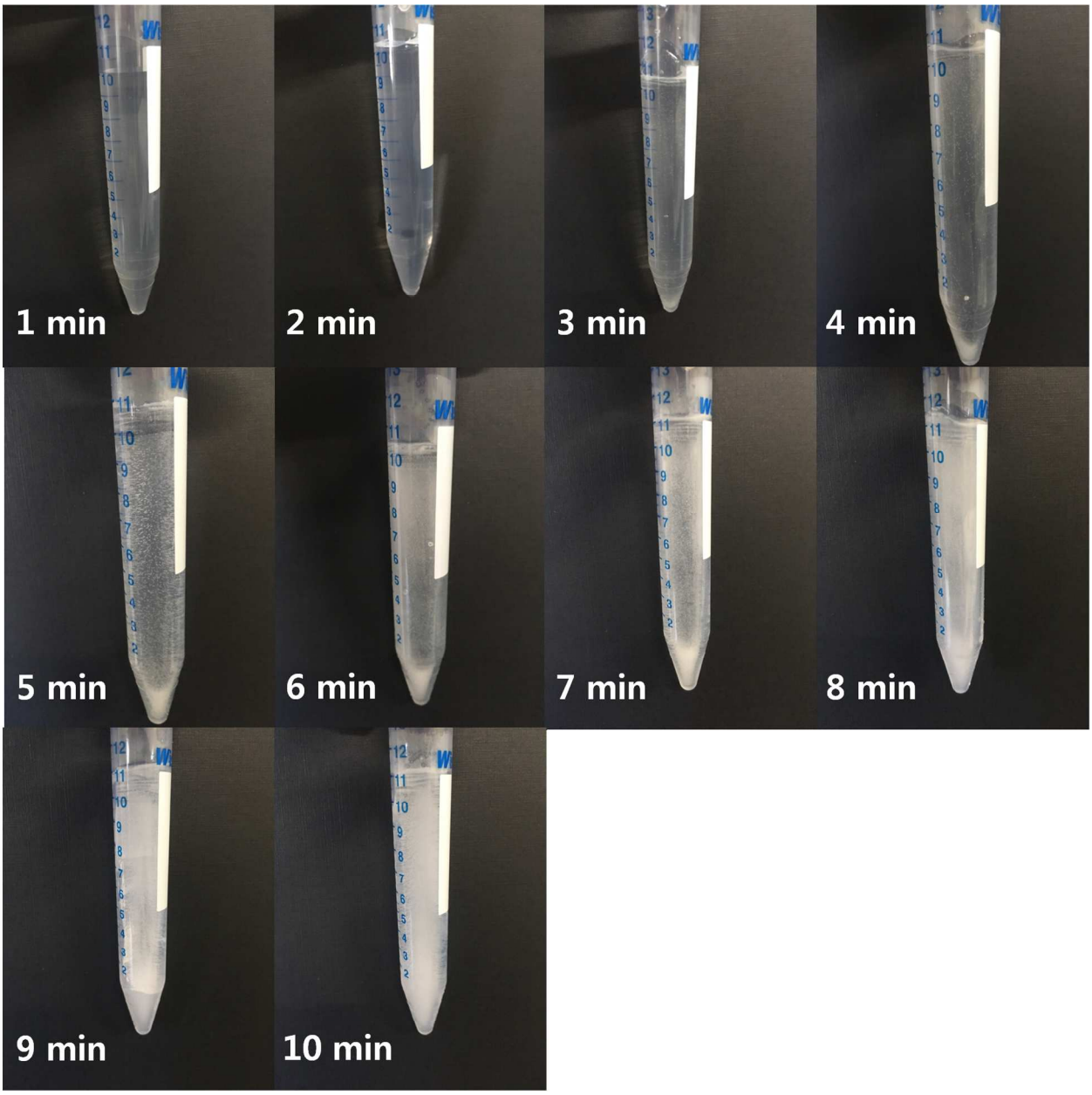

Figure S3. Degree of solidification of the solution containing IO_4^- and FFA as a function of reaction time. Experimental conditions were as follows: [IO_4^-] = 100 μM, [FFA] = 20 μM, pH = 3.0, and freezing temperature = −20 °C.

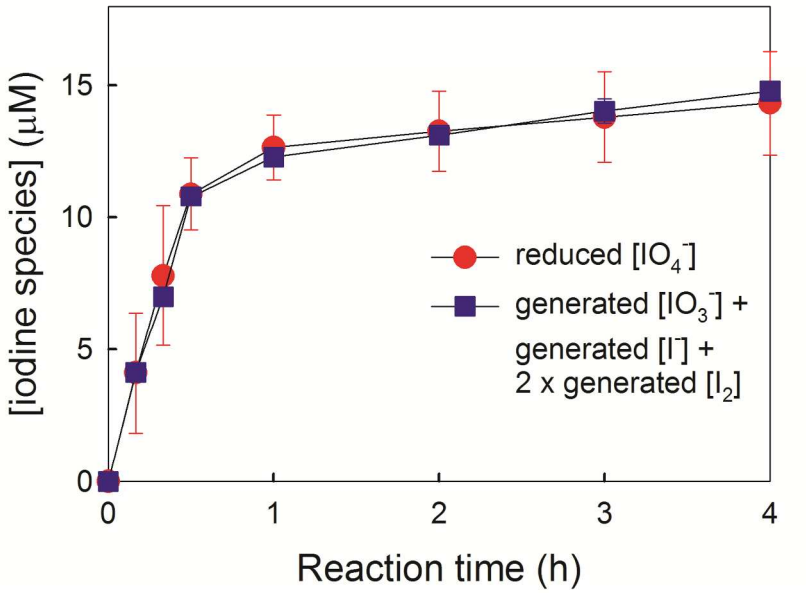

Figure S4. Total iodine mass balance (i.e., reduced $[IO_4^-]$ vs. generated $[IO_3^-]$ + generated $[I^-]$ + 2 × generated $[I_2]$) in the course of FFA degradation by IO_4^- (IO_4^- reduction by FFA) during freezing. Experimental conditions were as follows: $[IO_4^-]$ = 100 μM, [FFA] = 20 μM, pH = 3.0, and freezing temperature = −20 °C.

$H_5IO_6 \leftrightarrow H_4IO_6^- + H^+$, $pK_{a1} = 1.64$ (S1)

$H_4IO_6^- \leftrightarrow H_3IO_6^{2-} + H^+$, $pK_{a2} = 8.36$ (S2)

$H_3IO_6^{2-} \leftrightarrow H_2IO_6^{3-} + H^+$, $pK_{a3} = 12.20$ (S3)

$H_4IO_6^- \leftrightarrow IO_4^- + 2H_2O$, $K_D = 40$ (S4)

$2H_3IO_6^{2-} \leftrightarrow H_2I_2O_{10}^{4-} + 2H_2O$, $K_X = 141\ M^{-1}$ (S5)

Equilibria among various iodine^{VII} species, where pK_{a1}, pK_{a2}, and pK_{a3} are the acid dissociation constants, and K_D and K_X are dehydration and dimerization constants, respectively.[1]

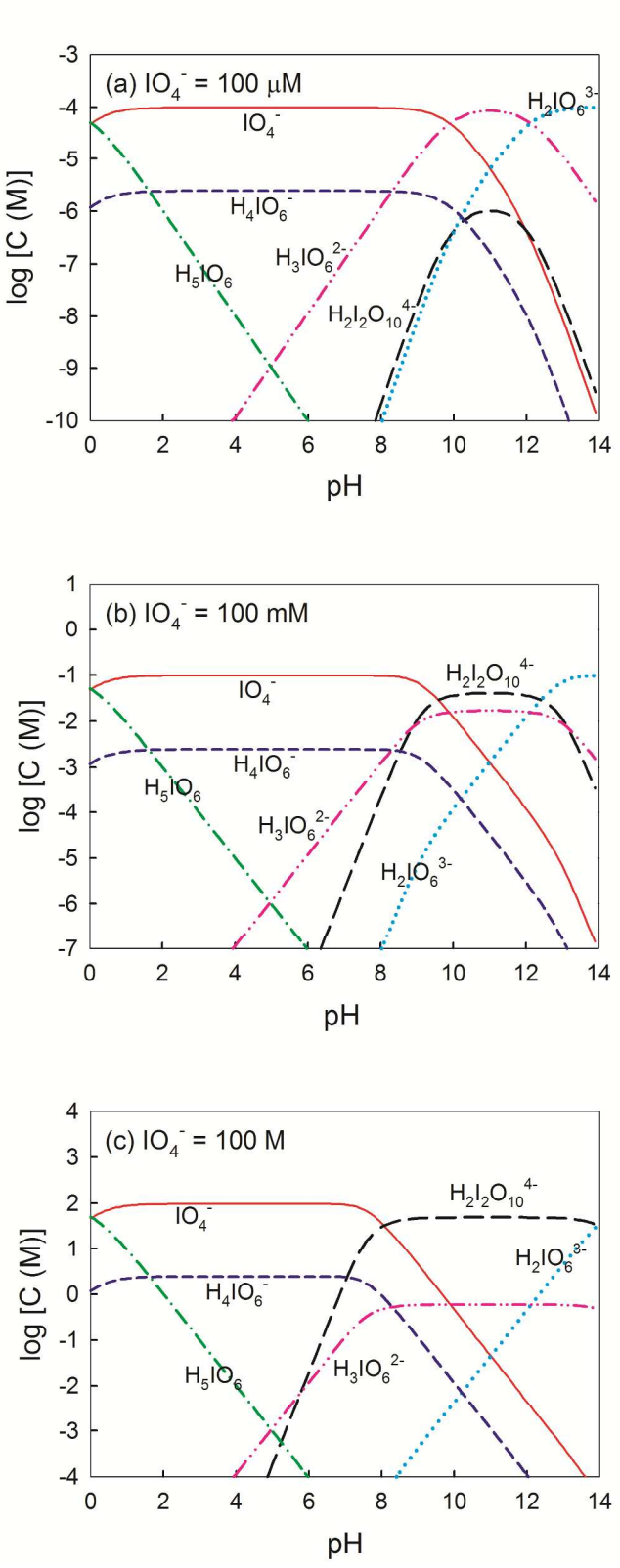

Figure S5. pH-dependent speciation of IO_4^- at [IO_4^-] = (a) 100 μM, (b) 100 mM, and (c) 100 M.

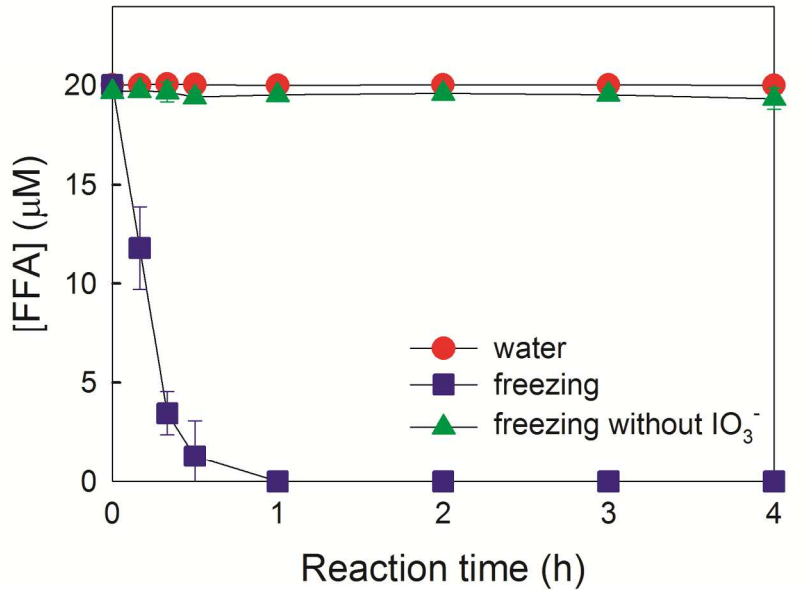

Figure S6. Degradation of FFA in the presence of IO_3^- in water and during freezing. Experimental conditions were as follows: [IO_3^-] = 100 μM, [FFA] = 20 μM, pH = 3.0, water temperature = 25 °C, and freezing temperature = −20 °C.

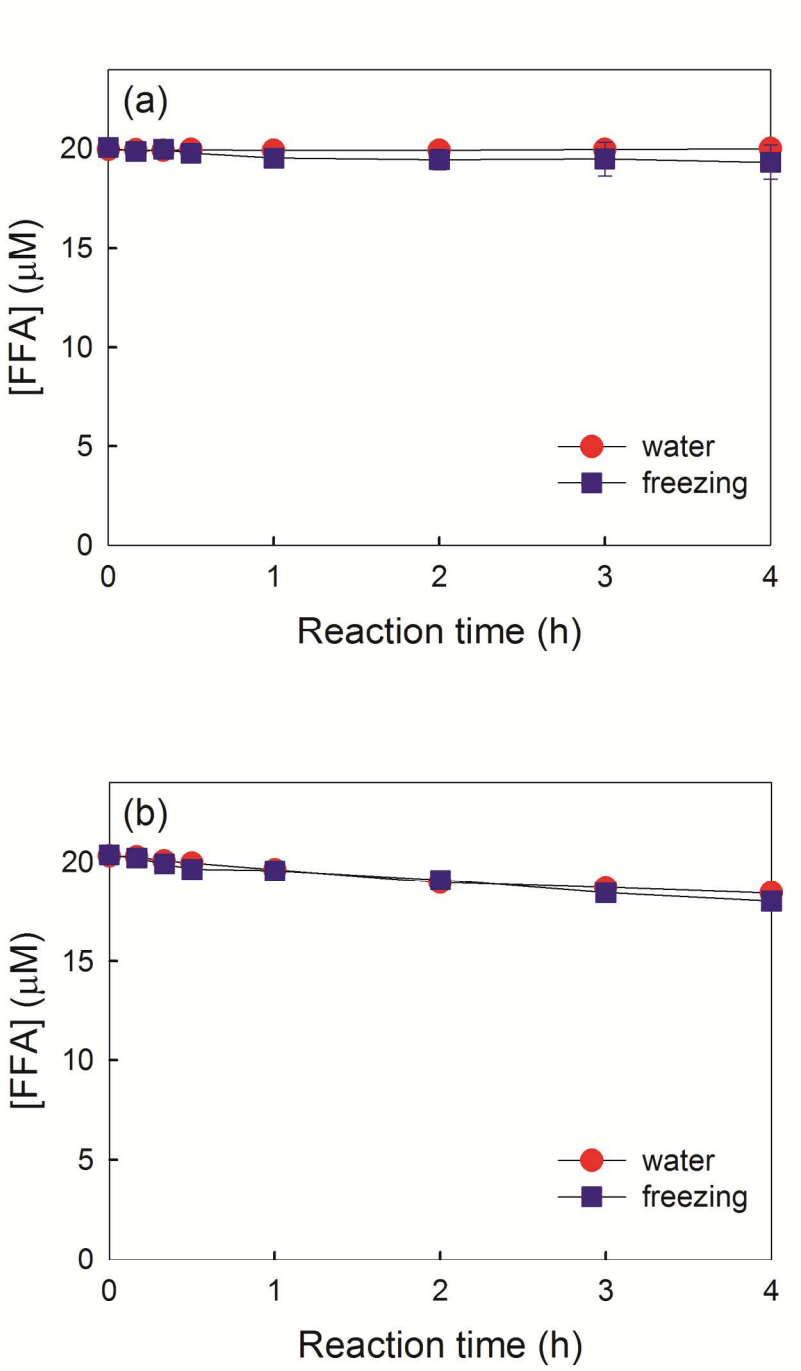

Figure S7. Degradation of FFA in the presence of (a) I^- and (b) I_2 in water and during freezing. Experimental conditions were as follows: [I^-] = 100 μM for part a, [I_2] = 100 μM for part b, [FFA] = 20 μM, pH = 3.0, water temperature = 25 °C, and freezing temperature = −20 °C.

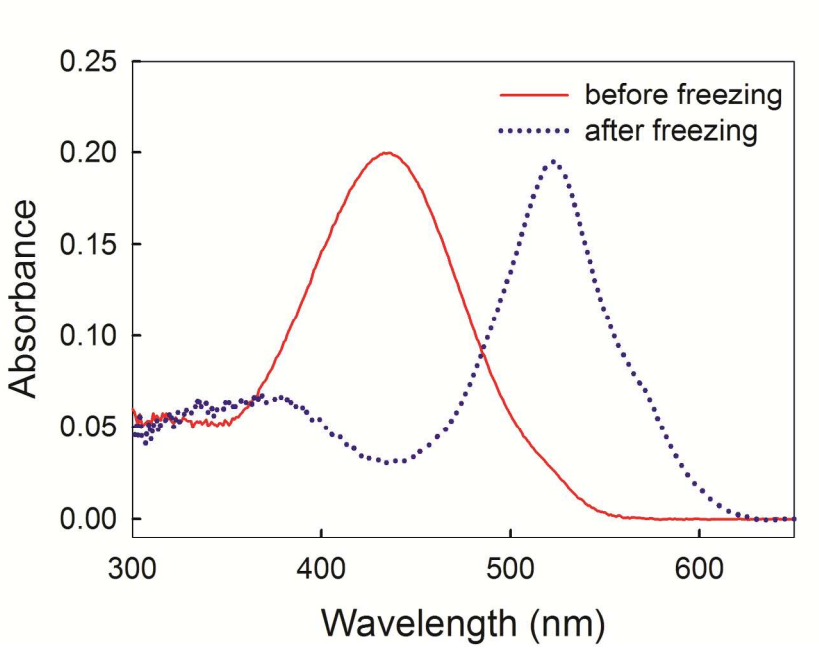

Figure S8. UV−visible absorption spectra of CR as an in situ pH probe before and after freezing the aqueous solution of IO_4^- and CR. Experimental conditions were as follows: [IO_4^-] = 100 μM, [CR] = 20 μM, pH = 3.0, water temperature = 25 °C, and freezing temperature = −20 °C.

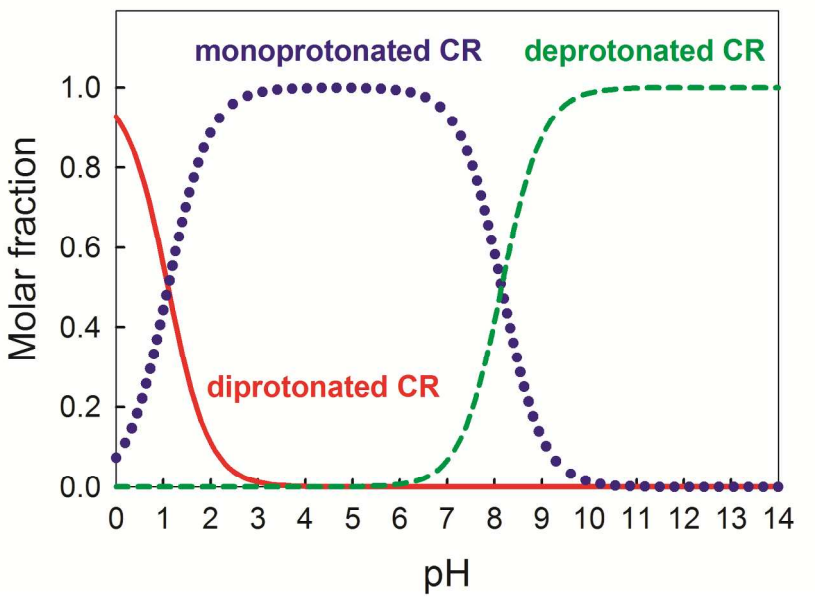

Figure S9. pH-dependent speciation of cresol red (CR). The acid dissociation constants (pK_a) of CR were obtained from references 2 and 3 (pK_{a1} = 1.10 and pK_{a2} = 8.15).

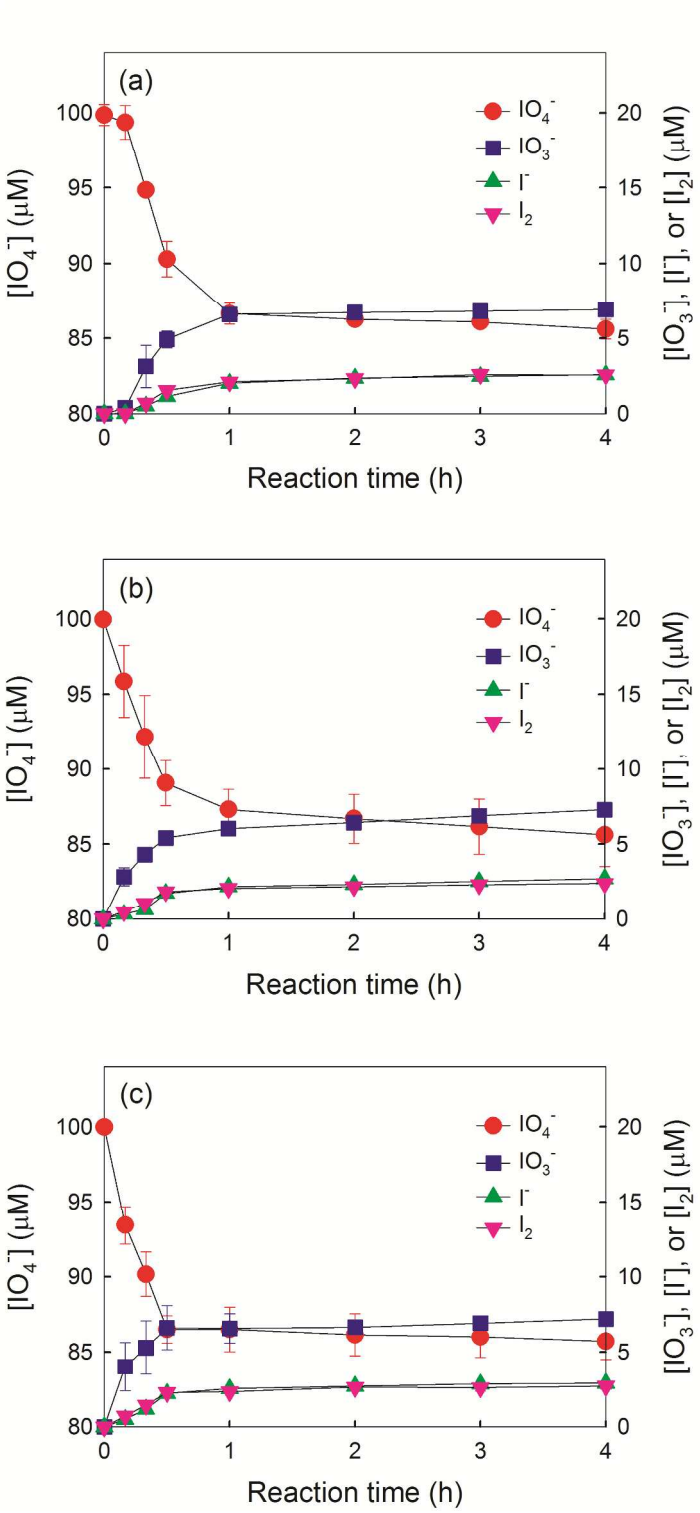

Figure S10. Reduction of IO_4^- by FFA and the concurrent production of IO_3^-, I^-, and I_2 during freezing at (a) −10 °C, (b) −20 °C, and (c) −30 °C. Experimental conditions were as follows: $[IO_4^-]$ = 100 μM, [FFA] = 20 μM, and pH = 3.0.

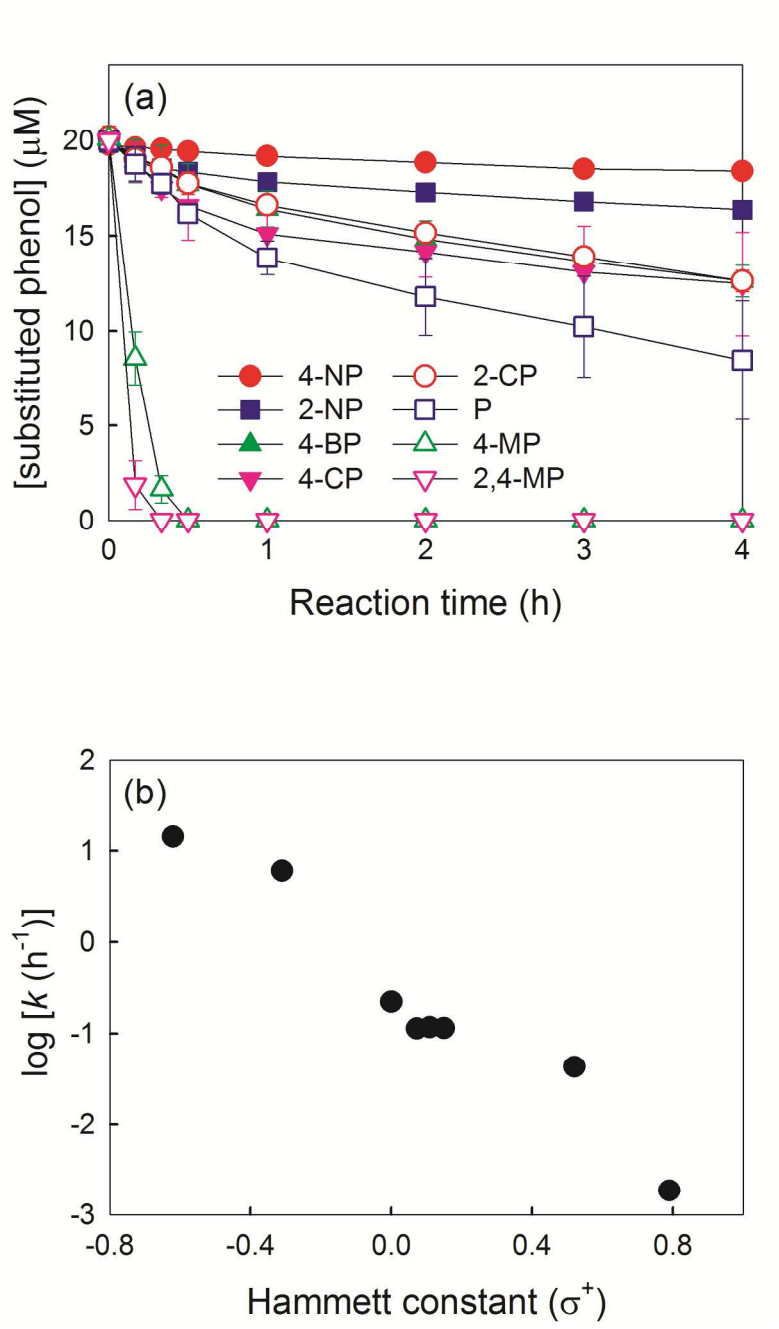

Figure S11. (a) Degradation of various substituted phenols (4-nitrophenol (4-NP), 2-nitrophenol (2-NP), 4-bromophenol (4-BP), 4-chlorophenol (4-CP), 2-chlorophenol (2-CP), phenol (P), 4-methylphenol (4-MP), and 2,4-dimethylphenol (2,4-MP)) in the presence of IO_4^- during freezing. (b) Correlations between degradation rate constants (k) and Hammett constants (σ^+). Experimental conditions were as follows: [IO_4^-] = 100 μM, [substituted phenol] = 20 μM, pH = 3.0, and freezing temperature = −20 °C. The Hammett constants of the substituted phenols were obtained from references 4 and 5.

Discussion on the effect of cooling method on the induction period. The freezing-induced degradation of FFA in the presence of IO_4^- is initiated when the aqueous solution is almost solidified (i.e., when the concentrations of IO_4^-, FFA, and protons reach the minimum level for inducing the degradation process). Therefore, the cooling rate (i.e., the solidification rate) is a key factor in determining the induction period. The aqueous solution is solidified more rapidly when a substance with higher specific heat capacity and density is used as a coolant. The specific heat capacity (C_p) of ethanol is twice that of air (2.0 kJ/kg·°C for ethanol vs. 1.0 kJ/kg·°C for air). The density of ethanol (l) is much higher than that of air (g) (827.0 kg/m^3 for ethanol vs. 1.4 kg/m^3 for air). In addition, the circulation of cold ethanol in a cryogenic ethanol bath contributes to the rapid solidification of the aqueous solution. These can help explain why the induction period in outdoor experiments is much longer than that in laboratory experiments.

References

(1) Weavers, L. K.; Hua, I.; Hoffmann, M. R. Degradation of triethanolamine and chemical oxygen demand reduction in wastewater by photoactivated periodate. *Water Environ. Res.* **1997**, *69*, 1112-1119.

(2) Perrin, D. D. Buffers of low ionic strength for spectrophotometric p*K* determinations. *Aust. J. Chem.* **1963**, *16*, 572-578.

(3) Dean, J. A. *Lange's Handbook of Chemistry*, 14th, ed.; McGraw-Hill: New York, 1992.

(4) Lee, Y.; Yoon, J.; von Gunten, U. Kinetics of the oxidation of phenols and phenolic endocrine disruptors during water treatment with ferrate (Fe(VI)). *Environ. Sci. Technol.* **2005**, *39*, 8978-8984.

(5) Guan, C.; Jiang, J.; Pang, S.; Luo, C.; Ma, J.; Zhou, Y.; Yang, Y. Oxidation kinetics of bromophenols by nonradical activation of peroxydisulfate in the presence of carbon nanotube and formation of brominated polymeric products. *Environ. Sci. Technol.* **2017**, *51*, 10718-10728.